

5. Martian Dust Storms and Their Effects on Propagation

5.1 Introduction

One of the most remarkable features of Mars is the dust storm. Thus, there are some concerns about dust storm effects on radio wave propagation. We know that Mars has only one third of Earth's surface gravity and that the Martian surface atmospheric pressure is about 1/100 that of Earth. The wind speed at Mars is not significantly larger than at Earth. Thus, a question is how the wind at Mars can frequently raise enough dust to form a storm. To address this question, some wind-tunnel experiments have been performed.

On Earth particles around 0.08 mm in diameter are those most easily moved by the wind [Bagnold, 1941]. Above this diameter, larger wind speeds are required to overcome the inertial resistance due to the particle mass. The threshold velocities on Mars are much larger than those on Earth because of the thinner atmosphere. A wind-tunnel study [Greeley et al., 1980] showed that the optimum size for particle movement on Mars is near 0.1 mm, close to the size for Earth. Figure 5-1 shows that the threshold shear velocities (V_t) required to move the 0.1-mm particles range from 1.4 m/s for a 10-mb atmospheric pressure to 2.1 m/s for a 5-mb atmospheric pressure. On Earth threshold velocities at the optimum size are close to 0.2 m/s.

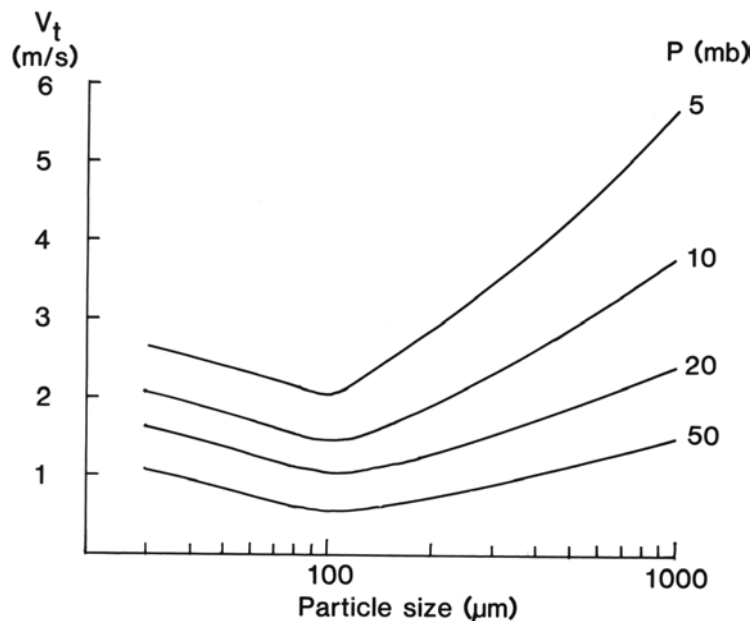


Figure 5-1. Threshold Velocities for Initiation of Particle Movement as a Function of Particle Diameter. The data are from wind-tunnel studies at four pressure levels representative of conditions at the Martian surface (adapted from Greeley et al. 1980).

There is a long history of Mars dust storm observations using terrestrial telescopes. Data on earlier storms have been reviewed by Slipher [1962] and Capen [1971]. Observations after 1971 are particularly well documented in Martin [1976] and Briggs et al. [1979]. Global or great dust storms are most common when Mars is near perihelion. Yellowish dust clouds were extensively

photographed during the oppositions of 1920–1922. This period of maximum insolation occurs in late southern spring near $L_s \sim 250^\circ$, where L_s is the aerocentric longitude of the Sun as measured in a Mars-centered fixed coordinate system, often used as an angular measure of the Mars year ($L_s = 90^\circ$, 180° , and 270° corresponding to the beginning of southern winter, spring, and summer, respectively).

Spacecraft such as Mariner 9, Vikings 1 and 2, Mars Pathfinder, and MGS, have provided direct observations of Martian dust storms. Most of these dust storms occur in spring and summer in the southern hemisphere, in particular along the periphery of the South polar cap. When seasonal heating of the surface and atmosphere induces convection of sufficient strength to raise dust from the surface, the large temperature contrasts drive thermal circulation radially away from the higher ice covered area. These downslope winds are a possible source for dust storms. The great dust storms typically originate as localized dust clouds in the southern temperate zone. These storms expand slowly over a few days, after which they may either decline or rapidly intensify into global dust hazes that may obscure the entire planet. Most of the storms move with velocities of 14–32 m/s and dissipate within a few days. Afterward, the atmosphere usually takes a few weeks or months to become clear. Dust storms can reach as high as 60 km.

Figure 5-2 shows a local dust storm near the edge of the south polar cap imaged by Mariner 9. This fascinating image shows dust swirling over a large area. Martian global dust storms tend to start in the southern hemisphere with a local dust storm, such as the one shown here. Local dust storms seem to be swept into huge storms that envelope the entire planet, as was discovered by the Mariner 9 mission in 1971 and Viking missions to Mars in the 1970's. During 1977 the Viking spacecraft, both orbiters and landers, made extensive observations of dust activity. Between the two global dust storms, numerous local dust storms were observed. Figure 5-3 shows one of the local dust storms observed by the Viking orbiter camera.

Global dust storms do not seem to occur every Martian spring or summer, however. The action of sand carried by winds during Martian global dust storms makes a great contribution toward wearing down rocks on the Martian surface. Martian dust storms are generally divided into three types:

- (1) Local dust storms—clouds and hazes with a spatial dimension < 2000 km
- (2) Regional dust storms—clouds and hazes with a spatial dimension > 2000 km
- (3) Planet-encircling—dust storms that encircle the whole planet at some latitude

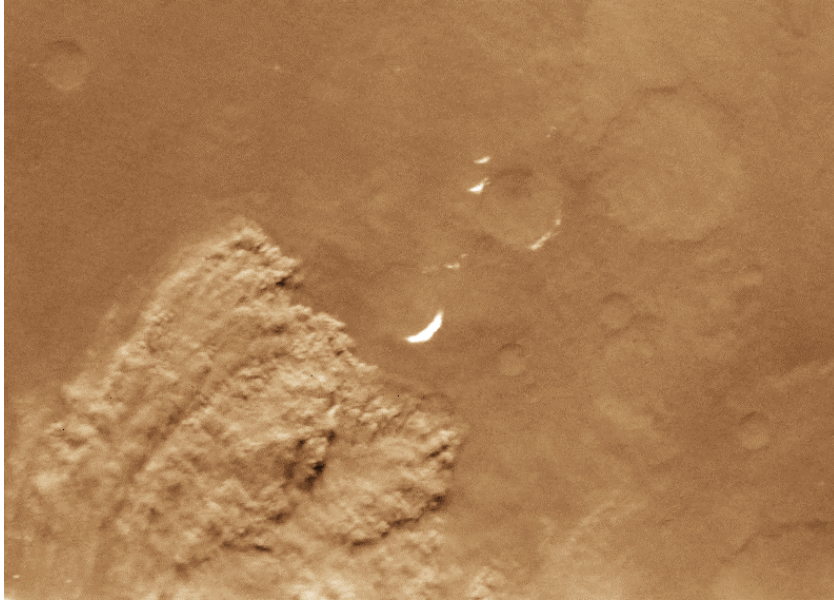


Figure 5-2. A Local Dust Storm Observed by Mariner 9 at the Edge of the South Polar Ice Cap, Just Visible at the Lower Right. The time is that of perihelion, $L_s = 250^\circ$.

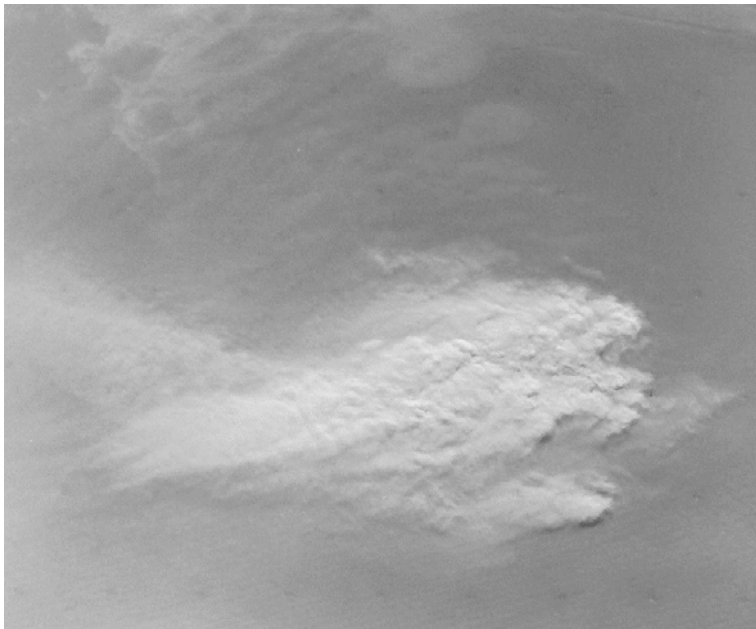


Figure 5-3. A Local Dust Storm in the Solis Planum Region at $L_s = 227^\circ$. The season is mid-southern spring, between the two 1977 global storms.

5.2 Local and Regional Dust Storms

Local and regional dust storms are relatively common on Mars. They tend to occur in areas of high topographic and/or high thermal gradients (usually near the polar caps) where surface winds would be strongest. It is believed that large temperature differences between the icy polar regions and warmer dark regions of lower latitudes drive the polar dust storms. This type of storm is usually several hundreds of kilometers in extent and is located near the edge of the south polar cap. Some local storms grow larger, others die out. The Martian north polar cap is another region of dust storms.

Observations of the Sun using the camera on Mars Pathfinder showed more dust in the Martian atmosphere than was expected. In fact, the amount of dust was comparable to Viking observations during clear (non-dust-storm) times. The measurements were made by taking images of the Sun in different colors and with the Sun at different elevations in the sky. As the Sun went lower in the sky, the light passed through more dust, becoming fainter and fainter, and indicating the amount of dust. Martian dust includes magnetic, composite particles, with a mean size of one micron.

On April 12, 1998, the Mars Orbiter Camera (MOC) of the Mars Global Surveyor detected a large local dust storm in the original Viking Lander 1 region as shown in Figure 5-4. This view, a map projection, shows an image area of about 310 km wide by 290 km, at a scale of 300 m (985 ft) per pixel. A well-developed local dust storm dominates this view of the planet. Plumes from the storm suggest that the wind is blowing from the lower left towards the upper right. The slightly dark zone around the dust cloud may be a surface that has been swept clean of a fraction of the mobile dust. The dust cloud obscures most of the landing site as seen in this image.

The MOC detected a large, regional dust storm in Noachis Terra on November 26, 1997. The dust storm is the large cloudy feature near the southern polar frost cap that can be seen at the bottom of Figure 5-5. The 1997 dust storm was different from that of 1977. The 1977 storm was first observed at $L_s = 205^\circ$ in the Thaumasia region; it expanded rapidly through the southern hemisphere and then into the northern hemisphere, whereupon dust was observed at both Viking landing sites. During 1997 the southern hemisphere remained clear until after $L_s = 220^\circ$. Subsequently, considerable dust was seen over and around the cap as well as in Noachis. This dust storm never became global, but it was large enough (greater than 2,500 km (1,550 miles) in size) that it would have covered a third of the continental United States. MOC monitored this big dust storm into December 1997. It was most intense between November 26 and December 2, then faded into a haziness that persisted for several weeks. This effect was detected by the Mars Global Surveyor spacecraft during its aerobraking passes [Malin et al., 1998].



Figure 5-4. Dust Storm Picture Taken by MGS Orbiter Camera (MOC) During Orbit 235 Observations at 22.48°N, 47.97°W. The spacecraft was about 640 km from the surface with a view angle of 31.64°.

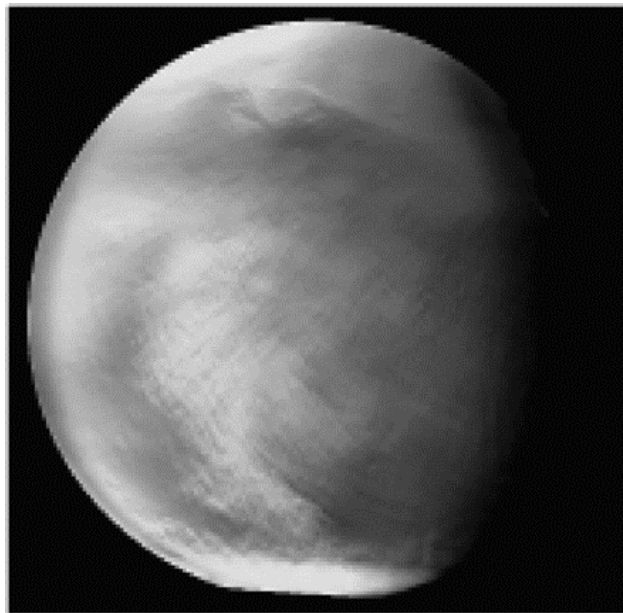


Figure 5-5. A Regional Dust Storm Observed by MGS Orbiter Camera (MOC) from Orbit 50 and $L_s = 251^\circ$ (Malin et al., 1998). The Storm extended from 25° to 60° N latitude and from 15°W to 40°E longitude, a distance of 2500 km.

5.3 Global Dust Storms

These storms are also called great dust storms or planet-encircling dust storms. We have listed the observed great storms in Table 5-1 [Zurek, 1982; Martin, 1984]. Before the 1971, all observations were made by terrestrial telescopes during each of the most favorable oppositions. Although local dust storms have been observed on Mars during all seasons, the global dust storms have not been observed to originate during northern spring or summer. Global dust storms have a profound impact on Martian environment evolution, such as dust deposits, aeolian processes, sediment features, atmospheric composition, atmospheric circulation, etc. [Christensen, 1986; Greeley et al., 1992; Haberle et al., 1982; Owen et al., 1977; Pollack et al., 1977; Zurek et al., 1992].

Table 5-1. Martian Great Dust Storms

| Year | Observation | L _s (°) | Initial Location |
|-------------|------------------|--------------------|------------------|
| 1909 (Aug) | Earth | | |
| 1911 (Nov) | Earth | | |
| 1922 | Earth | 192 | |
| 1924 (Oct) | Earth | | |
| 1924 (Dec) | Earth | 237 | Isidis Planitia |
| 1939 | Earth | | Utopia |
| 1941 (Nov) | Earth | | South of Isidis |
| 1943 | Earth | 310 | Isidis |
| 1956 | Earth | 250 | Hellespontus |
| 1958 | Earth | 310 | Isidis |
| 1971 (July) | Earth | 213 | Hellespontus |
| 1971 (Sept) | Earth, Mariner 9 | 260 | Hellespontus |
| 1973 | Earth | 300 | Solis Planum |
| 1977 (Feb) | Viking | 205 | Thaumasia |
| 1977 (June) | Viking | 275 | |
| 1979 | Viking | 225 | |

Two global dust storms occurred in 1977 and were extensively observed by the two Viking landers and two orbiters [Kahn et al. 1992; Zurek, 1982]. The first storm developed in the Thaumasia region at L_s = 205°. Initially, the storm was seen as a large but localized disturbance resembling other local storms. By the second day, the storm had spread to cover an area thousands of kilometers wide. Visibility improved in 6 or 7 weeks. The second storm apparently developed at L_s = 275° in the same area of the planet as the first storm. It seemed to be a more intense storm than the first one. Figure 5-6 shows the expansion process of the second 1977 storm [Kahn et al., 1992].

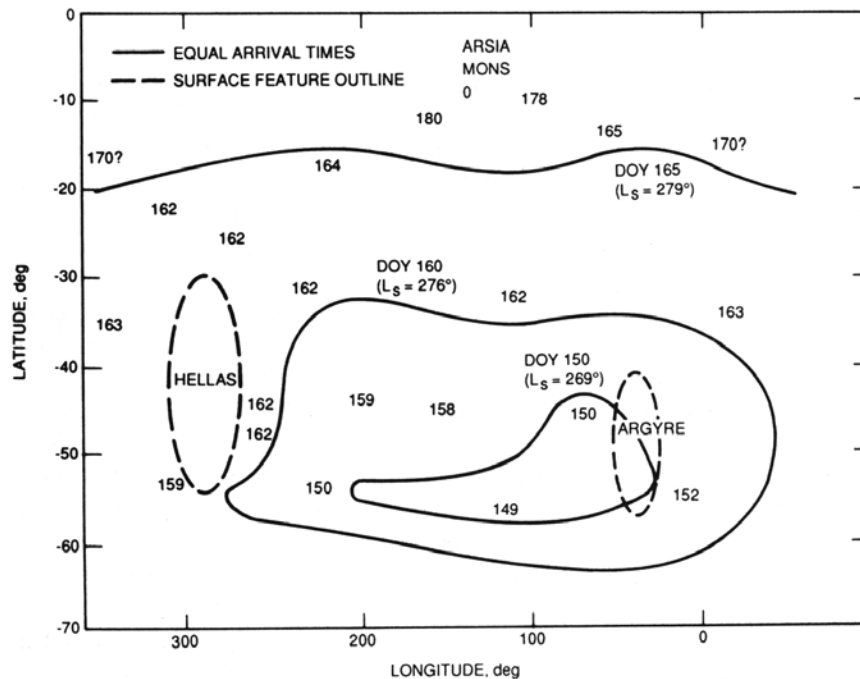


Figure 5-6. Expansion of the June 1977 Storm, as Derived from Viking Orbiter Visual Imaging. Arrival dates of maximum opacity change are shown in day of year, 1977; areocentric longitude L_s is given in parentheses (adopted from Kahn et al., 1992).

A number of local dust storms were observed between the clearing of the first storm and the start of the second. The two Viking landers carried cameras capable of determining the line-of-sight extinction opacity of the atmosphere. Figure 5-7 shows visible optical depth measured by Viking Lander 1 for the two storms. The opacity of a global haze inferred from surface pressure data [Zurek, 1981] has values similar to the optical depths derived from Sun-diode measurements [Colburn et al., 1989]. During the same period the Martian surface pressure had obvious increases that can be correlated with the opacity changes resulting from direct atmospheric heating by the dust.

5.4 Effects on Radio Wave Propagation

5.4.1 Dust Storm Parameters

Mars dust is thought to consist of basalt and montmorillonitic clay. Clear atmosphere corresponds to a background aerosol loading of optical depth ranging from 0.3 to 0.5, at a wavelength of 0.67 μm , while during the most intense portions of the global storms the opacity was found to increase to 4.0–5.0. A local storm generally has a spatial extent of several hundred kilometers. A great dust storm can have a size as big as the state of Texas, or even cover half the planet. Although a storm can reach as high as 50-km altitude, its cloud can be equivalent to a slab with 10-km thickness [Smith and Flock, 1986] because the dust density decreases with increasing altitude. The total amount of dust along a ray path is

$$\int_0^{\infty} N_0 e^{-\frac{z}{H_d}} dz = N_0 H_d \quad (5-1)$$

where H_d is the dust scale height (~ 10 km) and N_0 is the surface dust density.

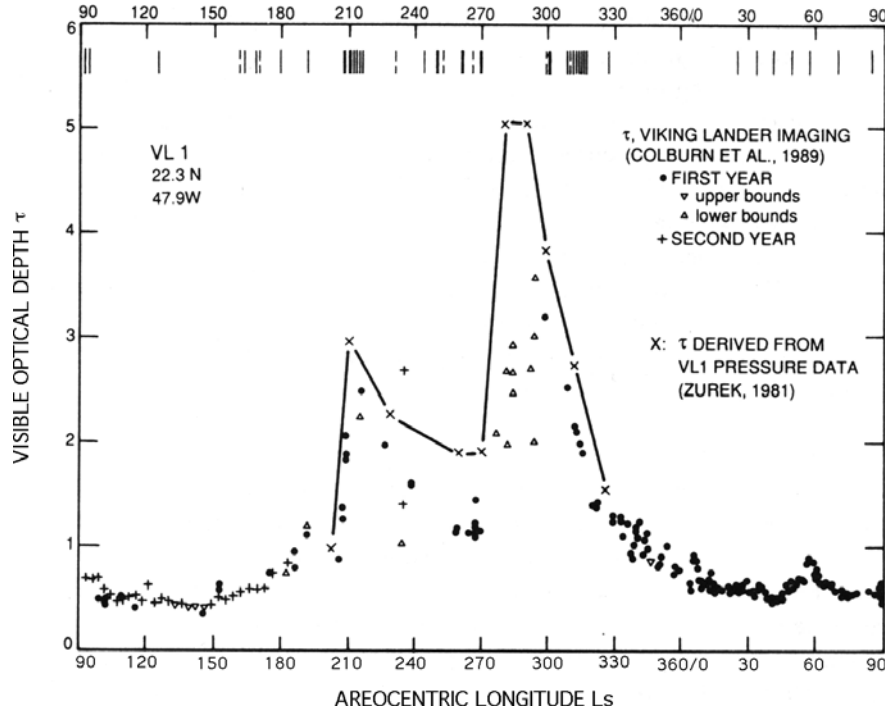


Figure 5-7. Visible Optical Depths Derived from Viking Lander 1 Measurements (Colburn et al., 1989). Line indicates the opacity of a global haze inferred from Viking Lander 1 surface-pressure data (Zurek, 1981). Initial appearance or detection of all dust storms is indicated by vertical bars at the top.

Dust size distribution has been modeled using a modified gamma function [Toon et al., 1977; Hunt, 1979]:

$$N(r) = cr^{\alpha} \exp[-(\alpha/\gamma)(r/r_m)^{\gamma}] \quad (5-2)$$

where c is a normalization constant, $\alpha = 2$, $\gamma = 0.5$, and r_m is mean particle radius. Toon et al. [1977] found that $N(r)$ remained reasonably constant throughout the period of the 1971–1972 storms. There is very limited information about dust size. On the basis of the study of Pollack et al. [1979] in assessing the Martian atmospheric opacity during both clear periods and during dust storms, the average dust size is estimated to be on the order of 1–4 μm . Currently we do not understand why Martian dust has such small average size, as compared with Earth. This size of particle is extremely difficult to set into motion by wind, as shown in the experimental results of Greeley et al. [1980].

The refractive index of Martian dust has also been derived based on knowledge of terrestrial dust. Actually the real and imaginary parts of the mean permittivity ($\varepsilon = \varepsilon' + j \varepsilon''$) of dust particles depend on the radio wave frequency, and on the composition, size, and moisture of the dust. In Table 5-2, we list some values that were used in the previous studies.

Table 5-2. Dielectric Permittivity Index of Dust Particles

| Index ε | 10 GHz [*] | 10 GHz Clay | 10 GHz Sand | S Band ^{**} | 32 GHz Clay ^{***} | 8.8 GHz Clay ^{***} | Dust at 20 μ m ^{***} | Dust at 2 μ m ^{***} |
|------------------------|-----------------------------|------------------------------|-------------------------|-------------------------|-------------------------------|--------------------------------|--------------------------------------|-------------------------------------|
| ε' | 4.56 (+0.11, -0.24) | 7.42 (+1.73, -1.22) | 3.35 (± 0.03) | 4.56 | 2.5 | 2.5 | 2.0 | 3.0 |
| ε'' | 2.51 (+0.074, -0.066) | 1.119 (+0.597, -0.437) | 0.042 (± 0.02) | 0.251 | 0.06 | 0.02 | 0.4 | 0.1 |

* Ghobrial [1980]

** Goldhirsh [1982]

*** Smith and Flock [1986]

5.4.2 Radio Wave Attenuation through Dust Storms

Sand or dust particles can cause attenuation of radio waves through the scattering and absorption by particles. When the particle size is smaller than the wavelength, Rayleigh scattering theory applies. When the particle has a size larger than the wavelength, we should use Mie scattering theory to calculate effective refractive index [Flock, 1987].

For terrestrial sand or dust storms, the visibility, V , is often used to describe the distance at which a mark disappears against the background. Storms usually have a visibility of 10 m or less, with a minimum of 3.8 m, and can reach a height of 1 km or more [Bagnold, 1941; Ghobrial, 1980; Ansari and Evans, 1982]. Dust particles have an average size of 10 to 20 μ m, with the largest in a range of 80–300 μ m. For an extreme case, with a particle number density, N_T , of $10^8/\text{m}^3$, and dust material mass density, ρ , $2.6 \times 10^6 \text{ g/m}^3$, mass loading can reach 40–60 g/m^3 . At S-band (10^a cm wavelength), over a 20-km one-way path, attenuation can be as great as 13 dB. X-band (10 GHz) attenuation can reach 44 dB over the same path. Thus, in desert areas, sand storms can cause a problem for domestic-satellite services. Chu [1979] and Goldhirsh [1982] have summarized the studies of the effects of Earth dust storms on radio wave propagation. The microwave attenuation $A(\lambda)$ is given by:

$$A(\lambda) = \frac{189r}{\lambda V} \left[\frac{3\varepsilon''}{(\varepsilon'+2)^2 + \varepsilon''^2} \right] \quad (5-3)$$

where $A(\lambda)$ is in dB/km, V is visibility in kilometers, r is particle radius in meters, and λ is wavelength in meters.

Smith and Flock [1986] performed the first study of radio wave propagation through Martian dust. The computation method is essentially that of Chu [1979] but uses observed maximum optical depth ($\tau = 6$) at 0.67 micron wavelength rather than visibility for Martian dust storms. Under an assumption that a Martian dust cloud is equivalent to a slab with a scale height H_0 (about 10 km) thickness, attenuation may be expressed as

$$A(\lambda) = 54.62 \frac{r\tau}{\lambda} \left[\frac{3\epsilon''}{(\epsilon'+2)^2 + \epsilon''^2} \right] \quad (5-4)$$

where τ is the optical depth, which is a measure of the dust cloud opacity and is defined in the following. For vertical illumination, $I = I_0 e^{-\tau}$, I is the signal intensity at the surface, while I_0 is the intensity with no attenuation. Smith and Flock [1986] found that for a worst case estimate (particle size of 20 μm), the total attenuation for 32 GHz (Ka-band) is about 1.3 dB, relatively small. However, they did not explain why there is a significant difference between Mars' dust attenuation and Earth's, even though both values of N_T and ρ for dust storms are similar in both planets.

When a distribution of particle size is available, we can use another type of expression [Goldhirsh, 1982]:

$$A(\lambda) = \frac{1.029 \times 10^6 \epsilon''}{\lambda[(\epsilon'+2)^2 + \epsilon''^2]} \sum_i N_i r_i^3 \quad (5-5)$$

where N_i is the number of particles with radii between r_i and $r_i + \Delta r_i$ per m^3 . Actually, the term $\sum_i N_i r_i^3$ gives the dust mass loading. Using a normalized particle-size probability distribution function from Toon [1977], we can integrate this equation to get a total attenuation effect as

$$A(\lambda) = \frac{3.087 \times 10^6 \epsilon'' N_T}{\lambda[(\epsilon'+2)^2 + \epsilon''^2]} \int_0^\infty N(r) r^2 dr \quad (5-6)$$

where N_T is the total particle density in $\#/\text{m}^3$ and $N(r)$ is the normalized particle number density at radii between r and $r + \Delta r$ as given in equation (5-2). We can also use the mean particle radius \bar{r} , to calculate attenuation:

$$A(\lambda) = \frac{1.029 \times 10^6 \epsilon''}{\lambda[(\epsilon'+2)^2 + \epsilon''^2]} N_T \bar{r}^3 \quad (5-7)$$

where \bar{r} is obtained through an integration over all sizes of particles in $N(r)$.

As a comparison, Table 5-3 lists dust storm parameters and recalculated radio wave attenuation on Earth and Mars. We find that the key difference in parameters is particle size. Because $A(\lambda) \propto N_T r^3$, a 10 times difference in size (10–40 μm at Earth versus 1–4 μm at Mars) results in a three-order-of-magnitude difference in attenuation. A 3-dB attenuation at Mars is a worst case estimate for 32-GHz signals over an equivalent 10-km dust cloud consisting of 10- μm radius particles. If a signal propagates obliquely, the attenuation value should be derived by dividing by $\cos\theta$, where θ is the angle between the ray and the vertical direction, or dividing by $\sin\psi$, where ψ is the elevation angle. At Mars there is much less mass loading as compared with Earth, but its dust number density is one third that of Earth.

Even though there is no direct optical visibility measurement available at Mars, we can use dust distribution to calculate the parameter

$$V = \frac{5.5 \times 10^{-4}}{N_T r^2} \quad (5-8)$$

Using $N_T r^2$ values deduced by Pollack et al. [1977, 1979], we find that Mars has a much greater visibility during its dust storms than the Earth.

The attenuation values at Table 5-3 are for Ka-band. However, we can scale the value into other wavelength bands using $A(\lambda) \sim 1/\lambda$. Shorter wavelength (higher frequency) signals undergo greater attenuation.

Table 5-3. A Comparison of Dust Storm Parameters Between Earth and Mars

| | N_T m^{-3} | ρ g/m^3 | Mean Size (μm) | Maximum Size (μm) | Visibility (m) | Path Length | Attenuation at 32 GHz | Mass Loading |
|-------|--------------------------|--------------------------|-----------------------------------|-----------------------------------|-------------------|----------------|--------------------------|----------------------|
| Earth | 10^8 | 2.6×10^6 | 30–40 | 80–300 | 5.1–3.8 | 10km | 65 dB | 40–60 g/m^3 |
| Mars | 3×10^7 | 3.0×10^6 | 1–10 | 20 | 184 | 10km | 3 dB | 0.4 g/m^3 |

5.5 Summary and Recommendations

Even though Mars has a thin atmosphere, Martian winds can frequently generate large dust storms. This happens especially during late spring or early summer seasons in the southern hemisphere, when Mars is at its perihelion. The southern hemisphere is suddenly heated, and a large temperature difference relative to the northern hemisphere is generated. This drives strong winds and dust from the southern hemisphere to the northern hemisphere. This process also has a profound impact on the Mars atmospheric environment and surface features.

A global dust storm has a size at least as big as the continental United States, and can cover most of the planet. Frequent local storms have a spatial extent of several hundred kilometers. Dust storms can reach altitudes as high as 50 km with an opacity of 4–6 (probably even 10). However, it is expected that Martian dust storms have relatively small attenuation effects on radio wave propagation because of the small dust particle sizes. At worst, Martian dust storms could have a

3-dB attenuation at Ka-band. For optical communication, attenuation will be much larger. Martian dust has a mean size of 1–10 μm , at least four times smaller than dust on Earth. We do not know why Martian winds can lift such small particles, while wind tunnel experiments show that particles with a size of 100 μm are the most favorable candidates.

To perform an accurate estimate of Martian dust storm attenuation on radio waves, we need detailed information, such as dust particle size distribution, composition, dielectric permittivity, and dust cloud dimensions. So far, we only have very limited knowledge about these parameters. Current values about particle dielectric permittivity is based on similar materials from Earth. For example, if the mean dust particle size increases to 20 μm , the attenuation will increase eight times. Thus, accurate knowledge of the particle size distribution is critical for attenuation calculations. We suggest an extensive measurement and study on Martian dust storms in future Mars missions.

We recommend that mission designers for any spacecraft landing in the southern hemisphere during the late spring or early summer seasons should consider dust storm effects on telecommunication, especially near the southern polar-hood region. Even though local dust storms can occur at any time during the year, and at any location, the most severe dust storms usually take place near the southern polar-hood region. During this period, optical communication is impossible, and Ka-band communications also suffer significant attenuation. We need to have adequate margins (e.g., 5 dB) for signal transmission.

References

- Ansari, A.J. and B.G. Evans, Microwave propagation in sand and dust storms, *Proc. IEE*, 129, Part F, 315, 1982.
- Bagnold, R.A., *The physics of blown sand and desert dunes*, Methuen London, 1941.
- Briggs, G.A., et al., Viking Orbiter imaging observations of dust in the Martian atmosphere, *J. Geophys. Res.*, 84, 2795, 1979.
- Capen, C.F., Martian yellow clouds-past and future, *Sky & Teles.*, 41, 117, 1971.
- Christensen, P.R., Regional dust deposits on Mars: Physical properties, age and history, *J. Geophys. Res.*, 91, B3, 3533, 1986.
- Chu, T.S., Effects of sandstorms on microwave propagation, *Bell Syst. Tech. J.*, 58, 549, 1979.
- Colburn, D., et al., Diurnal variations in optical depth at Mars, *Icarus*, 79, 159, 1989.
- Flock, W.L., *Propagation Effects on Satellite System at Frequencies below 10 GHz, A Handbook for Satellite System Design*, NASA Reference Publication 1108(02), 1987.
- Ghobrial, S.F., The effect of sandstorm on microwave propagation, *Proc. Nat. telecomm. Conf.*, Houston, TX, 2, 43.5.1, 1980.
- Goldhirsh, J., A parameter review and assessment of attenuation and backscatter properties associated with dust storms over desert regions in the frequency range of 1 to 10 GHz, *IEEE Trans. Ant. Propaga.*, AP-30, 1121, 1982.

- Greeley, R.R., et al., Threshold wind speeds for sands on Mars: Wind tunnel simulations, *Geophys. Res. Lett.*, 7, 121, 1980.
- Greeley, R. et al., Martian aeolian processes, sediments, and features, in *Mars*, edited by H.H. Kieffer et al., The University of Arizona Press, Tucson & London, 730, 1992.
- Haberle, R.M et al., Some effects of global dust storms on the atmospheric circulation of Mars, *Icarus*, 50, 322, 1982.
- Hunt, G.E., On the opacity of Martian dust storms derived by Viking IRTM spectral measurements, *J. Geophys. Res.*, 84, 8301, 1979.
- Kahn, R.A., et al., The Martian dust cycle, 1017, in *Mars*, edited by H.H. Kieffer et al., The University of Arizona Press, Tucson & London, 1992.
- Malin, M.C., et al., Early views of the Martian surface from the Mars Orbiter Camera of Mars Global Surveyor, *Science*, 279, 1681, 1998.
- Martin, L.J., 1973 dust storm on Mars: Maps from hourly photographs, *Icarus*, 29, 363, 1976.
- Martin, L.J., Clearing the Martian air: The troubled history of dust storms, *Icarus*, 57, 317, 1984.
- Owen, T., et al., The composition of the atmosphere at the surface of Mars, *J. Geophys. Res.*, 82, 4635, 1977.
- Pollack, J.B., et al., Properties of aerosols in the Martian atmosphere, as inferred from Viking lander imaging data, *J. Geophys. Res.*, 82, 4479, 1977.
- Pollack, J.B., et al., Properties and effects of dust particles suspended in the Martian atmosphere, *J. Geophys. Res.*, 84, 2929, 1979.
- Slipher, E.C., *The Photographic Story of Mars*, Flagstaff: Northland Press, 1962.
- Smith, E.K., and W.L. Flock, Propagation through Martian dust at X- and Ka-band, *TDA Progress Report 42-87*, Jet Propulsion Laboratory, Pasadena, CA, 291, July-September 1986.
- Toon, O.B., et al., Physical properties of the particles composing the Martian dust storm of 1971–1972, *Icarus*, 30, 663, 1977.
- Zurek, R.W., Inference of dust opacities for the 1977 Martian great dust storms from Viking Lander 1 pressure data, *Icarus*, 45, 202, 1981.
- Zurek, R.W., et al., Dynamics of the atmosphere of Mars, in *Mars*, edited by H.H. Kieffer et al., The University of Arizona Press, Tucson & London, 835, 1992.
- Zurek, R.W., Martian great dust storms: An update, *Icarus*, 50, 288, 1982.